Supporting Information

Synthesis of Mg/ Al Layered Double Hydroxides for Adsorptive Removal of Fluoride from Water: A Mechanistic and Kinetic Study

Gautam Kumar Sarma and Md. Harunar Rashid*

Department of Chemistry, Rajiv Gandhi University, Rono Hills, Doimukh 791 112,

Arunachal Pradesh, India

*Corresponding author e-mail: mhr.rgu@gmail.com

Characterization of the prepared materials. All the as-prepared LDHs were characterized by different spectroscopic, microscopic and diffractometric techniques. For X-ray diffraction study, the dried solid powder samples were used and the diffractograms were recorded in a Rigaku Ultima IV X-ray diffractometer using Cu k_α radiation with wavelength 0.154 nm. Fourier transforms infrared spectra (FTIR) of the powder samples were collected in a Thermo Scientific Nicolet iS5 spectrophotometer in the range of 4000 – 400 cm^{-1}. The pellets for recording the FTIR spectra were prepared by mixing the powder sample with dried KBr in the weight ratio of 1:100. For electron microscopic study, a small amount of the dry powder samples were spread on a carbon tape pasted on an aluminium stub and the micrographs were then recorded in a field emission scanning electron microscope (FE-SEM) (Carl Zeiss Sigma) at an accelerating voltage of 5 kV. For transmission electron microscopic (TEM) studies, a drop of aqueous suspension of individual powder sample was cast on a carbon coated copper grid. The excess solutions were soaked with a tissue paper followed by drying in air. The micrographs were then recorded in a high–resolution JEOL electron microscope (JEM 2100EM) at an accelerating voltage of 200 kV.

The nitrogen (N_2) gas adsorption–desorption isotherms of the LDHs were recorded at 77 K (Quantachrome Nova 1000 Instrument) after degassing the powder samples at 150 ºC for 4 h in an inert atmosphere. BET specific surface area and pore diameter was determined from the adsorption-desorption isotherms following the well-known Barrett-Joyner-Halenda (BJH) method. The thermal analysis of the powder samples were carried out on a thermogravimetric analyzer (Mettler Toledo TGA/ DSC 1, Star^e system) under N_2 atmosphere. Zeta potential measurement of the colloidal suspension of LDH was performed in a Malvern Zetasizer (Malvern Instruments; Nano-ZS) instrument. Atomic absorption spectroscopic (AAS) study on LDH sample was carried out on a Thermo Scientific AAS instrument (iCE-2500) in flame mode using air-acetylene/ nitrous oxide gas. X-ray photoelectron spectroscopy study was carried out on FEI PHI Versa Probe II Instrument using Al k_α source under ultra high vacuum condition.

Table S1: Experimental conditions for fluoride-LDH interactions

pH	4.0-10.0 (at unit interval)
Interaction time (min)	5, 10, 15, 20, 30, 45, 60, 90, 120, 150, 180, 240, 300, 360
Amount of LDH (g L^{-1})	1, 2, 3, 4, 5
Fluoride concentration (mg L^{-1})	2, 5, 7, 10, 15, 20, 25, 30
Temperature (K)	303 K

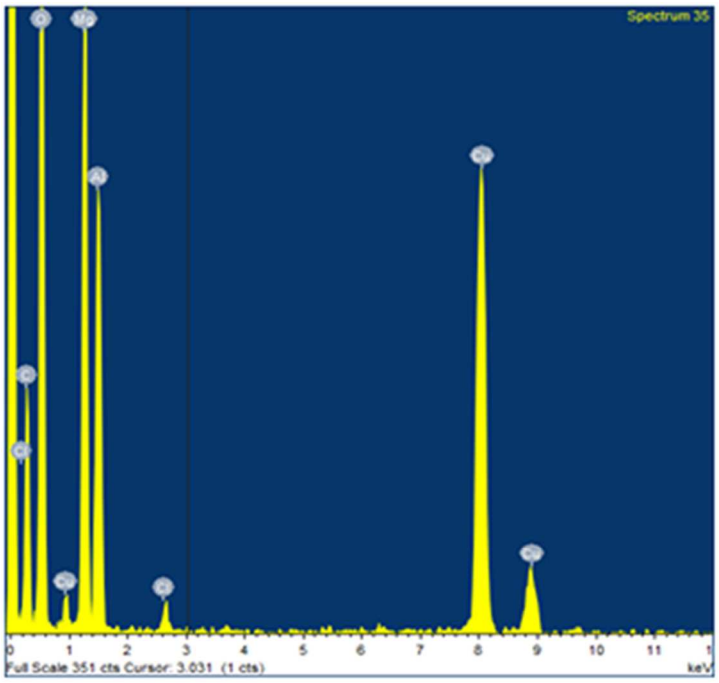

Figure S1. Energy dispersive X-ray spectra of LDH (sample Mg_Al-6).

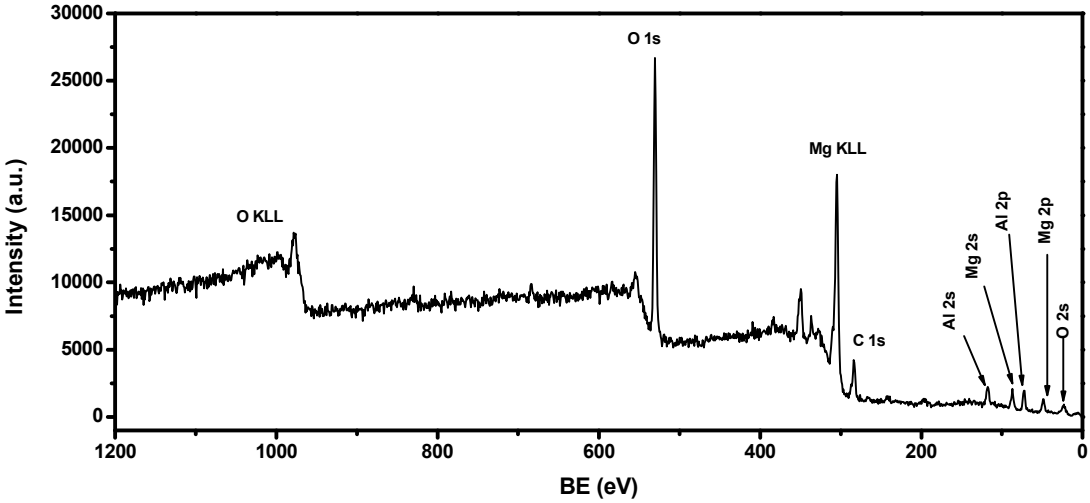

Figure S2. XPS survey scan spectrum recorded from sample Mg_Al-6.

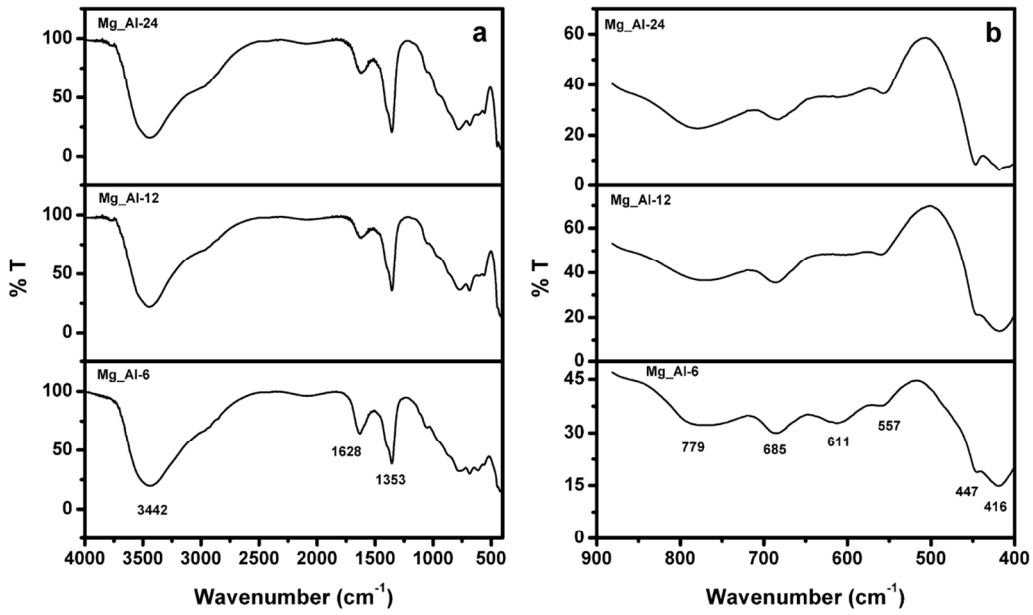

Figure S3. (a) FTIR spectra recorded from different LDH samples and (b) enlarged view of the region from 900 to 400 cm^{-1}.

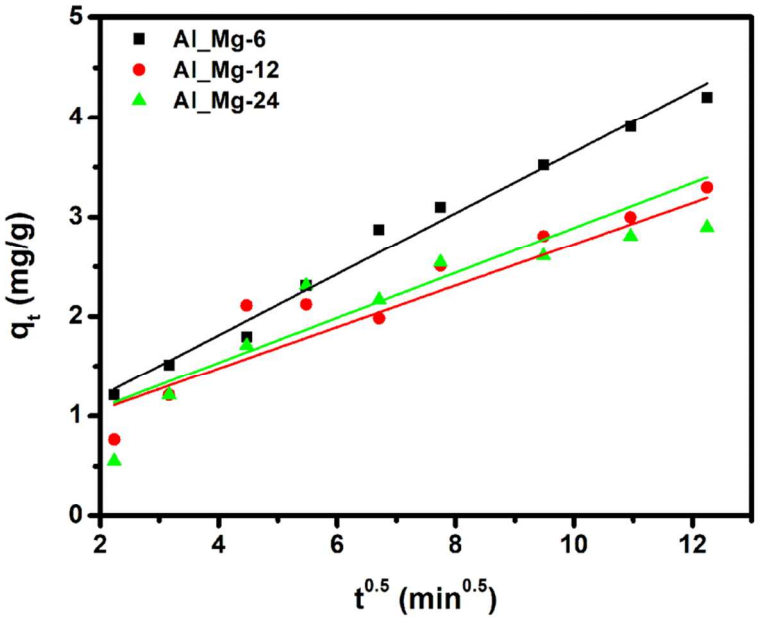

Figure S4. Plot showing the variation of q_t versus. $t^{0.5}$ on the basis of intra-particles diffusion rate equation.

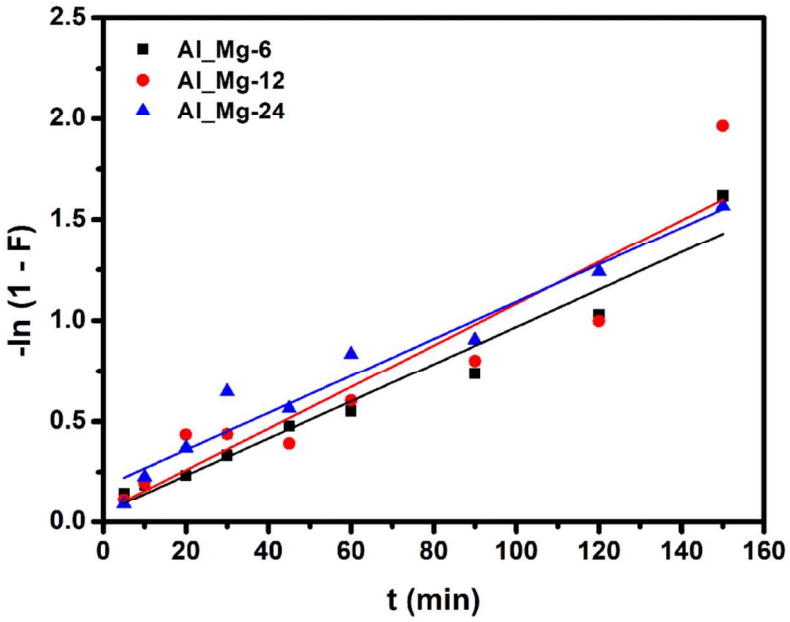

Figure S5. Plot showing the variation of – ln (1– *F*) versus *t* on the basis of liquid film diffusion model.

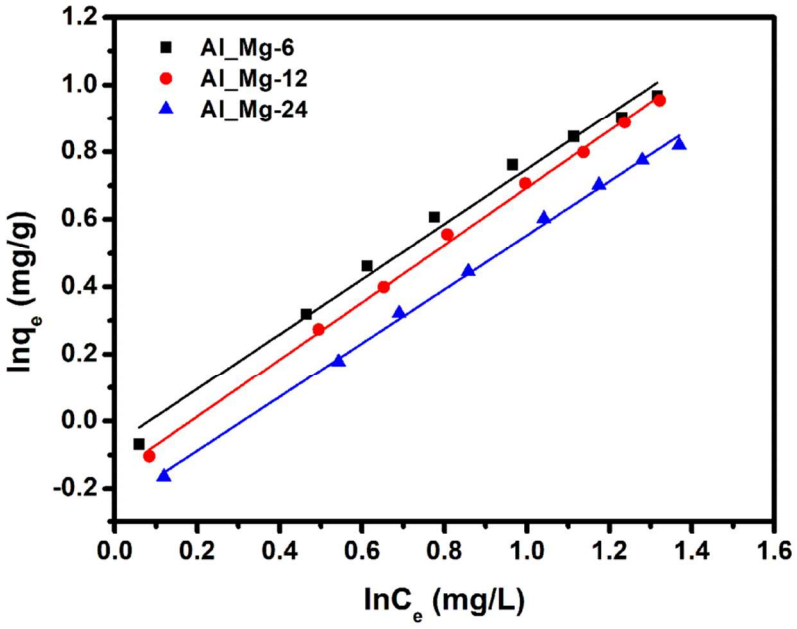

Figure S6. Plot showing the variation of ln q_e versus *ln* C_e on the basis of Freundlich adsorption isotherm.

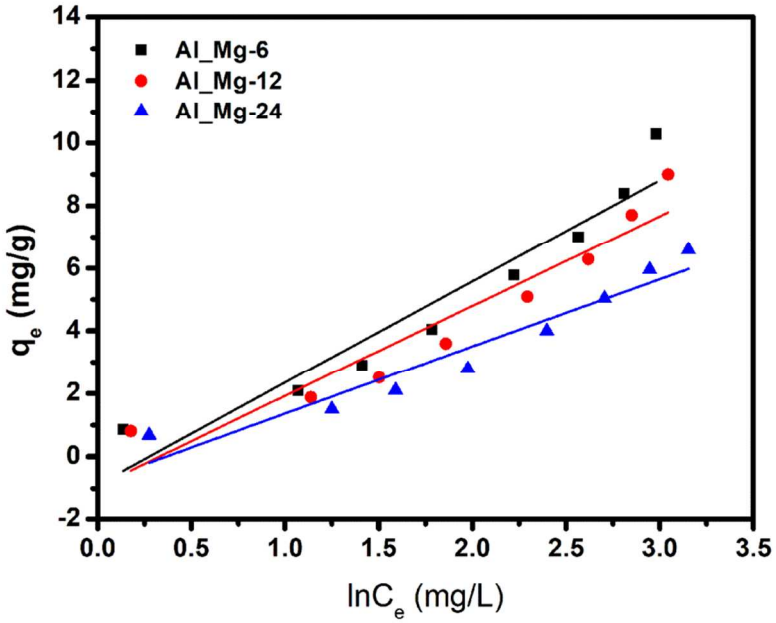

Figure S7. Temkin isotherm plots (q_e versus ln C_e) for fluoride adsorption on LDHs

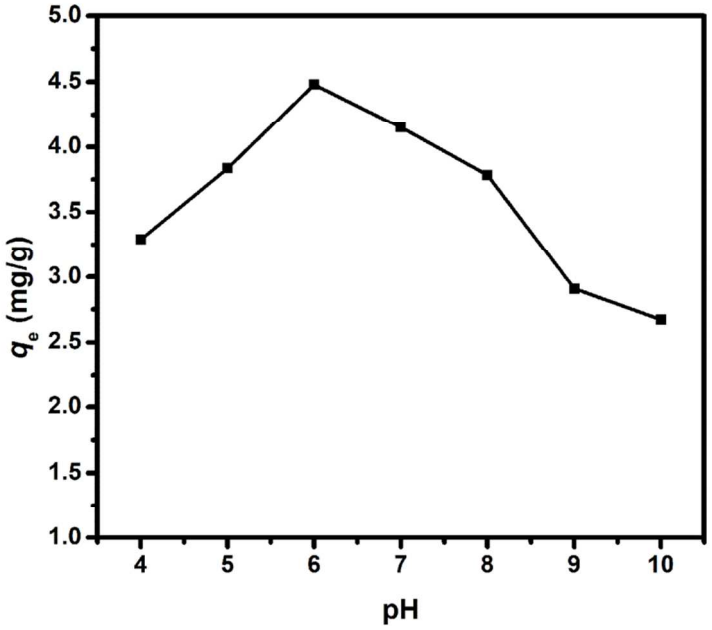

Figure S8. Effect of pH on adsorption of fluoride (10 mg L^{-1}) on LDH (sample Mg_Al-6).

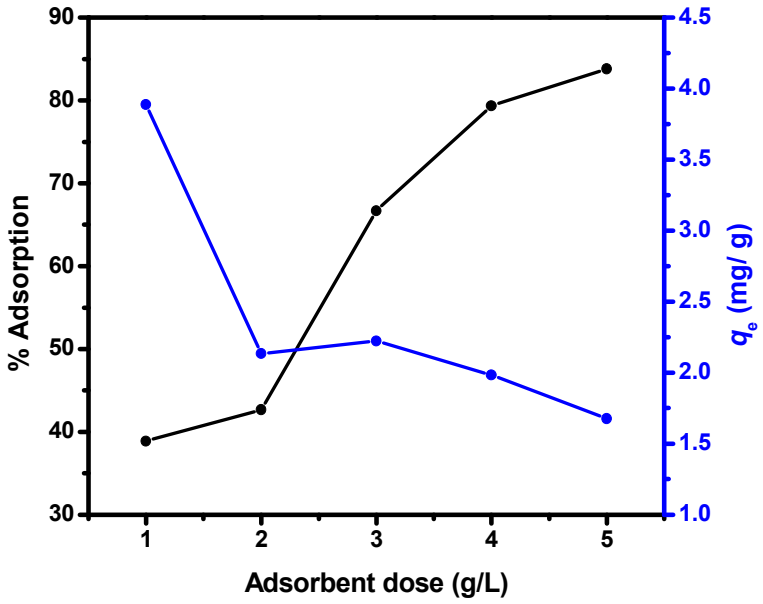

Figure S9. Plots showing the variations of %adsorption and effective adsorption, q_e of fluoride with dose of adsorbent.

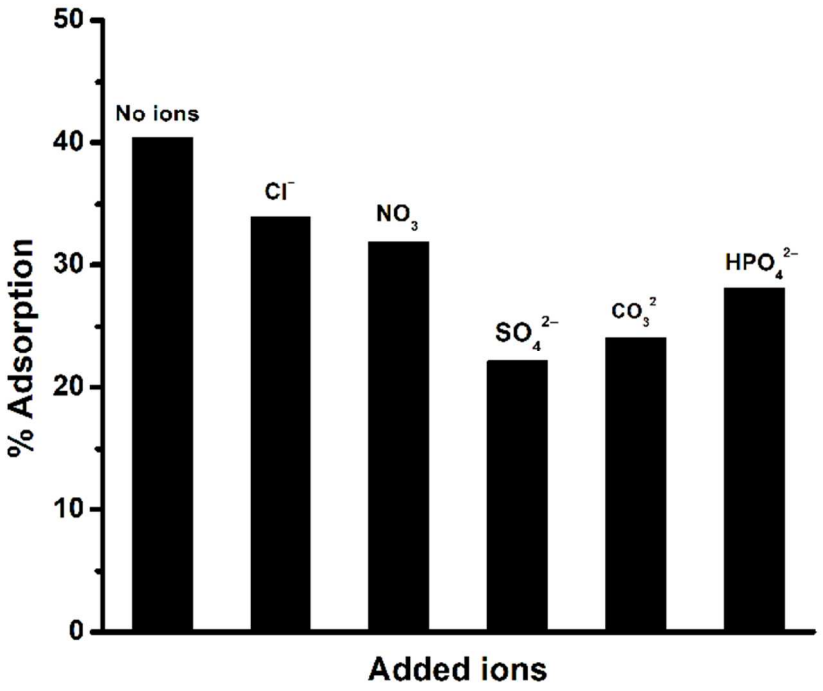

Figure S10. Variation of adsorption of fluoride in presence of different monovalent and bivalent anions.

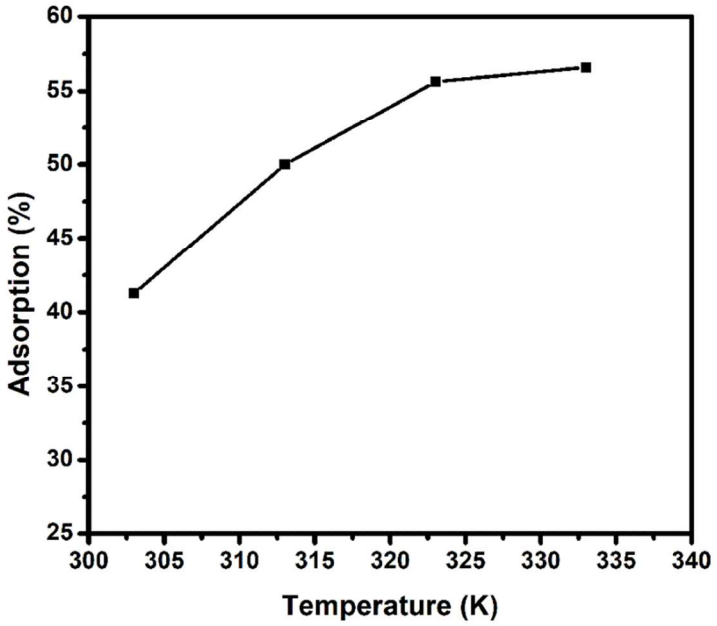

Figure S11. Variation of adsorption (%) with temperature for removal of fluoride by LDH.

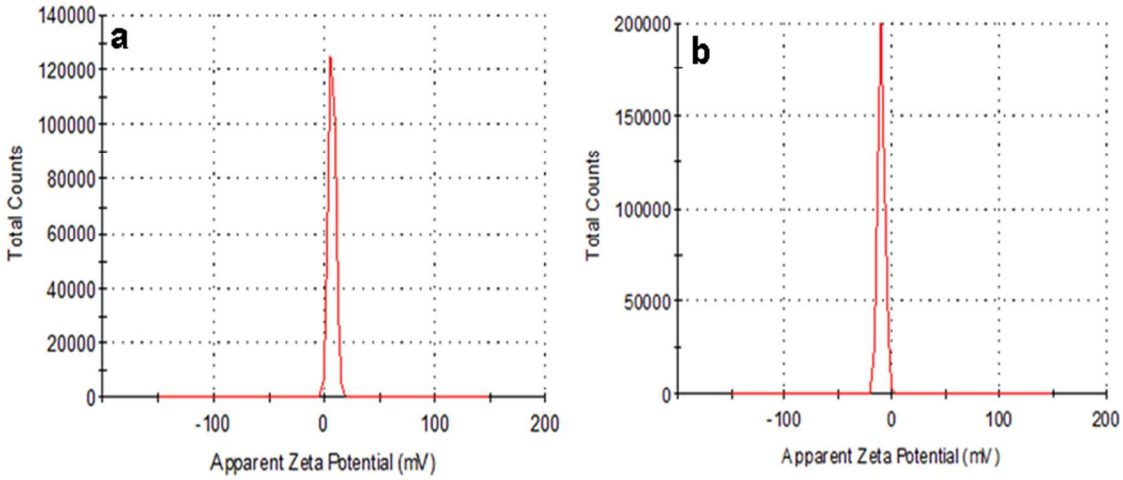

Figure S12. Zetal potential curves of LDHs (a) before and (b) after F^- ions adsorption.

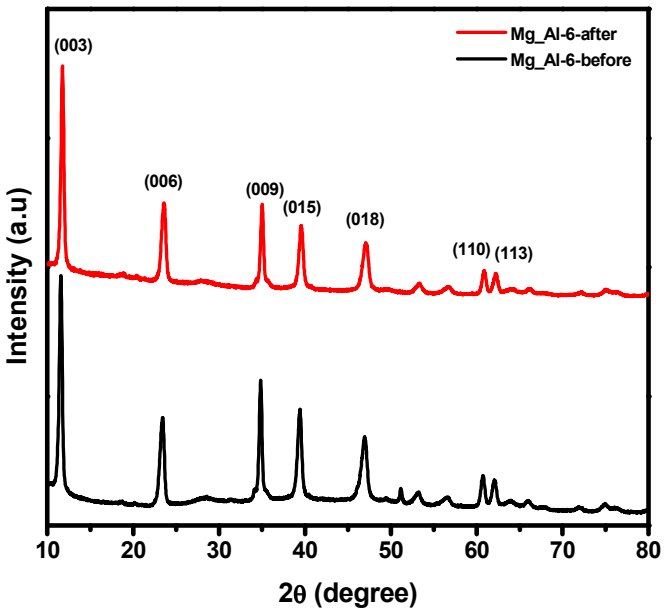

Figure S13. XRD patterns of LDH before and after fluoride adsorption.

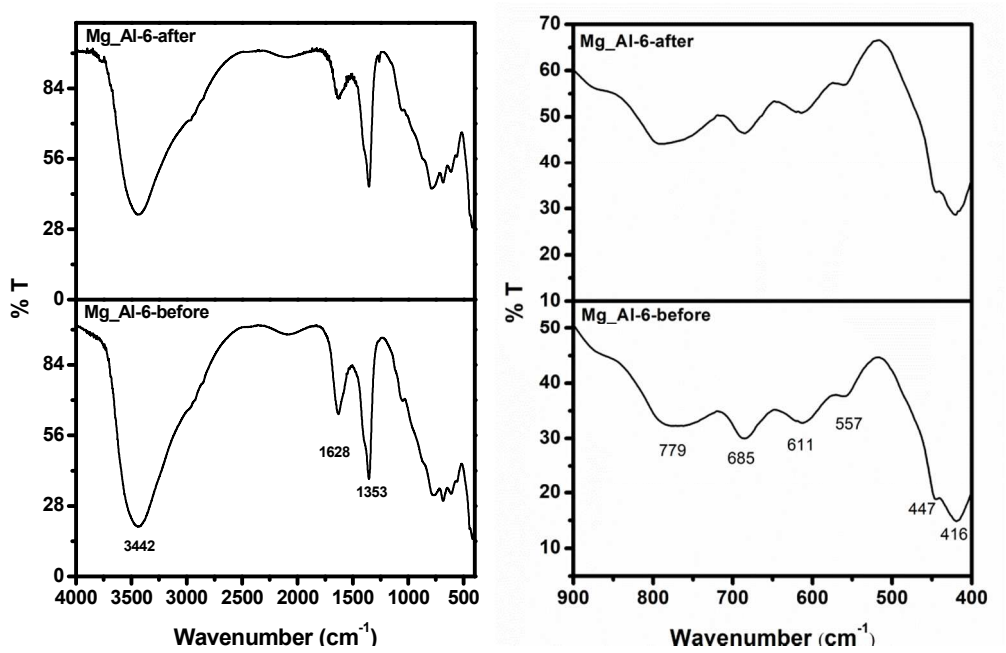

Figure S14. FTIR spectra of LDH before and after fluoride adsorption.

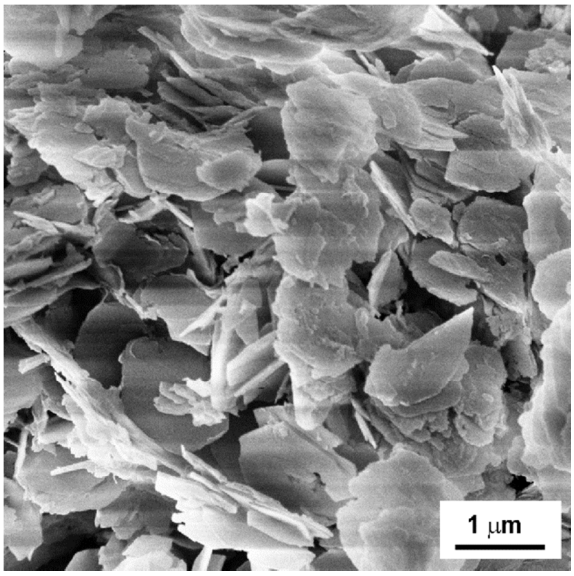

Figure S15. SEM images of recovered LDH (sample Mg_Al-6) after fluoride adsorption.